# Morpho-structural and Thermo-mechanical Properties of PA / fillers Nanocomposites for Industrial Applications

**ZINA VULUGA[1]\*, ION DINCA[2], ANA STAN[2], ION VOICU[3], CATALINA GABRIELA POTARNICHE[1], DAN DONESCU[1], CONSTANTIN RADOVICI[1], SEVER SERBAN[1], HORIA PAVEN[1], LIVIU DUMITRACHE[1], GABRIEL PRODAN[4]**

[1]National Research and Development Institute for Chemistry and Petrochemistry - ICECHIM, 202 Spl. Independentei, 060021, Bucharest, Romania
[2]National Institute for Aerospatial Research, 220 Iuliu Maniu Bd., 061126, Bucharest, Romania
[3]National Institute for Lasers, Plasma and Radiation Physics, Laser Department, P.O.Box MG-6, Bucharest, Romania
[4]Ovidius University of Constanta, 124 Mamaia Bd.,900527, Constanta, Romania

*Nanocomposites were obtained by dynamical melt blending. Some layered silicates and fillers based on nanocarbon were studied as nanofillers. The morpho-structural (XRD, HRTEM), thermal (TGA), dynamic-mechanical ($E_L$) and mechanical ($D_{ShD}$, $A_k$, $\sigma_p$) characteristics were examined. Nanocomposites with intercalated, partially exfoliated/partially intercalated and exfoliated lamellar structure with uniform dispersion of the nanofiller in the polyamide matrix were obtained. The nanocomposites exhibit thermal stability and improved properties as compared to the starting material.*

*Keywords: $PA_6$, nanocomposites, montmorillonite, nanocarbons*

Due to their exceptional properties the nanocomposites provide a potential route to producing special materials for industrial applications.

Polyamides are much used as technoplastics for structural applications. In the last years, many researchers tried to enhance polyamide properties by incorporating some nanomaterials (nanoparticles, nanotubes, nanofibers, fullerenes, nanowires) [1]. In general, nanomaterials are efficient reinforcing agents because of their very high aspect ratio. The uniform dispersion of anisotropic particles in a continuous polymer matrix may lead to a substantial improvement of matrix properties. When the mixing is done with components at nanometric scale, the obtained nanocomposites exhibit improved properties in comparison with conventional composites or individual polymers [2]. The nanocomposites properties are strongly influenced by the dimension of the constituent phases and the degree of the mixing between these phases. Depending on used components and the preparation method, composites with different properties may be developed, when a high adhesion at the polymeric matrix/filler interface is necessary [1]. Interfacial adhesion can be improved by specific interactions developed at polymer/ filler interface or by using particles with nanometer dimensions. This requirement could be achieved using surface modified filler and functionalized polymer [3, 4], or silane derivatives (coupling agents) [3, 5, 6].

The reaction of epoxy resin (EPON-828) with $H^+$, $NH_4^+$, or $[H_3N(CH_2)_{n-1}CH_3]^+$ cation-exchanged montmorillonite at a temperature in the range 200-300°C results in the polymerization of the epoxide and the concomitant delamination (exfoliation) of the clay structure [7].

Nearly exfoliated nanocomposites, with uniforme dispersed organophilic clay into $PA_6$ matrix were obtained through direct melt co-intercalation of epoxy resin and alkylammonium into Na-montmorillonite [8].

The laser synthesized carbon nanopowder and the layered silicate (montmorillonite) are largely used to obtain nanocomposites with improved mechanical, electrical or optical properties for different fields of application [9].

The effects of the nanofiller's types and of the dispersion procedure on polyamide/filler nanocomposites represents the essential aim of this work.

## Experimental part
### Materials

Organically modified montmorillonite with methyl tallow bis-2-hydroxyethyl ammonium chloride, as Cloisite 30 B (Cl 30 B), and with methyl dihydrogenated tallow ammonium sulfate, as Cloisite 93 A (Cl 93 A) (Southern Clay Products S.U.A.), with properties presented in table 1. Tallow composition is: fat acids with ~65% $C_{18}$; ~30% $C_{16}$; ~5% $C_{14}$. The silicate was dried 4 h at 80°C before utilization.

$H^+$ and $NH_4^+$ montmorillonites ($H^+$-MMT and $NH_4^+$-MMT), with properties presented in table 1, were prepared by ion exchange reactions of sodium montmorillonite obtained by purification of Romanian bentonite (with basal spacing $d_{001}$: 12.4 Å and 7% weight loss (TGA) in the temperature range of 20÷120°C). The sodium montmorillonite was dispersed 1% in distilled water at 90°C. An equal volume of solution containing HCl or $NH_4Cl$ in distilled water (0.1 mol/L) was added. Heating and stirring was continued for 30 min. After 72 h, at 70°C, in an oven with air circulation, the suspension was separated by centrifugation. The solid residue was washed with hot distilled water until no cloride ion was detected using the silver nitrate test. The product was dried at 60°C for 24 h, then milled in a ball mill.

Ropoxid P 401 (R), liquid epoxy resin type diglycidyl ether of bisphenol A modified with inert plastifier - dioctylphtalate, was manufactured by S.C. Policolor S.A., Romania.

Carbon nanopowder was synthesized by laser pyrolysis of a hydrocarbon-based acetylene/ ethylene (CNP 1) or benzene/ ethylene mixture (CNP 2) at the National Institute for Lasers, Plasma and Radiation Physics, Bucharest, Romania. This method is based on the interaction between laser radiation (continuous wave $CO_2$ laser) and at least one of the reactants. Depending on the gas mixture and experimental parameters, the synthesized nanocarbons

| Properties | Values | | | |
|---|---|---|---|---|
| | $H^+$-MMT | $NH_4^+$-MMT | Cloisite 93 A | Cloisite 30 B |
| Moisture, (%) | 8.5 | 6.8 | 1.0 | 1.9 |
| Loss at 700°C, (%) | 12.4 | 12.3 | 33.4 | 27.4 |
| Basal spacing, (Å) | | | | |
| -initial; | 13.4 | 12.1 | 25.7 | 18.0 |
| -after modification with R | 14.8 | 13.5 | 34.6 | 31.1 |

are composed by almost round nanoparticles with a size ranging from 10 to 50 nm and presenting different morphologies (turbostratic, fullerene-like or including long graphene ribbons). The experimental set-up and some of the carbon-based nanopowders were described elsewhere [10, 11].

Commercially available polyamide 6, pellets (PA) having 2.4-2.7 relative viscosity in $H_2SO_4$ 96.5% (manufactured by S.C. Sindfibre S.A., Romania), was dried, for 2 h at 105°C, prior to mixing.

*Treatment of $H^+$, $NH_4^+$ montmorillonite with epoxy resin*

The $H^+$ and $NH_4^+$ montmorillonite were mixed in a mill with Ropoxid P 401, at a 1:1 ratio, at room temperature. The mixture was then packed in an aluminum foil, and placed in an oven for polymerization of the epoxy resin and the concomitant delamination of the montmorillonite structure [7]. The polymerization - delaminating conditions were determined from DSC curves recorded under 50 cm³/min airflow on a Thermal Analysis Dupont 2100 at a heating rate of 20°C/min at 127°C and 5.5 min for $H^+$ montmorillonite - Ropoxid P 401 and at 201°C, 9 min for $NH_4^+$ montmorillonite - Ropoxid P 401. The $H^+$-MMTR and $NH_4^+$-MMTR respectively, with less ordered intercalated lamellar structure were obtained, suggested by the wider-rounded corresponding peaks and higher values for the $d_{001}$ (table 1).

*Treatment of organosilicate with epoxy resin*

Dynamical treatment of Cloisite 30 B and Cloisite 93 A with Ropoxid P 401 in a Brabender Plastograph was performed for 1h, at 80 °C and 100 rpm, at an organosilicate/epoxy resin ratio 5:1. Cl 30 BR and Cl 93 AR, respectively, with a more lamellar ordered structure (sharper peaks) and higher values for $d_{001}$ (table 1), due to the epoxy resin diffusion into the organosilicate galleries were obtained [8].

*Preparation of nanocomposites*

The PA/ organically modified-layered silicate nanocomposites were obtained under dynamical conditions, in a Brabender Plastograph, by incorporation of the modified organosilicate powder, either directly into the PA melt (DI), or by using a masterbatch of PA with 40% organically modified layered silicate (MB). This was diluted with PA until the final concentration of 5 % MMT, and mixed for 7 min in a 50 cm³ batch chamber at 235 ± 5 °C and 100 rpm. The obtained nanocomposites were marked as PA/ $H^+$-MMTR-DI, PA/ $NH_4^+$-MMTR-DI, PA/ Cl 30 BR-DI and PA/ Cl 93 AR-DI for the first procedure and as PA/ Cl 30 BR-MB and PA/ Cl 93 AR-MB for the second one.

The PA/carbon nanopowder composites were obtained also under dynamical conditions, in a Brabender Plastograph, by direct incorporation of 5% carbon nanopowder into PA melt, in the same conditions as those

for PA/organically-modified layered silicate nano-composites. The respective nanocomposites were marked as PA/ CNP 1 and PA/ CNP 2.

*Characterization*

The basal spacing was determined by means of X-ray diffraction (XRD) using a DRON-2.0 X-ray diffractometer with horizontal goniometry. The CuKα radiation source (λ = 1.5418Å) filtrated with Ni for $K_\beta$ component removing, in Bragg-Brentano system (by reflection) was used. The patterns were automatically recorded at small angles (2θ=2÷30°).

The weight loss of the analyzed samples, heated at constant rate, was determined with a Thermal Analysis Dupont 2100. The working conditions were: heating rate of 20°C/min, airflow of 50cm³/min and the temperature range from 0 to 700°C. The temperature at the maximum rate of weight-loss, on the decomposition steps, was determined by DTA curve.

The shape and the size of the nanoparticles were observed on Philips CM120ST instrument by High Resolution Transmission Electron Microscopy (HRTEM) coupled with selected area electron diffraction (SAED).

The dynamic-mechanical behavior was studied in the ultrasonic domain by using UNIPAN - 543 Material Tester, at the frequency of 1 MHz. The Apparent Dynamic Modulus of Elasticity, $E_L$, was determined in accordance to ASTM E 494, from the value of longitudinal speed of propagation of ultrasonic waves, $v_L$, and the density (in accordance to SR ISO 1183:1994), by using the relationship: $E_L = \rho \, v_L^2$.

The mechanical properties, Shore D Hardness ($D_{ShD}$), Unnotched Izod Impact Strength ($A_k$) at 23°C and Flexure Strength ($\sigma_i$), were determined in accordance to STAS 8643, SR EN ISO 180:2001 and ISO 14125, respectively.

**Results and discussions**

*PA/ organically modified layered silicate nanocomposites*

The XRD patterns presented in figure 1a reveal that with $H^+$ and $NH_4^+$ montmorillonite modified with epoxy resin, nanocomposites with intercalated/ partially exfoliated lamellar structure were obtained. The diffraction peaks at 2θ = 5.64° for PA/ $H^+$-MMTR-DI and at 2θ = 5.70° for PA/ $NH_4^+$-MMTR-DI nanocomposites are small (with greater breadths and lower intensities), practically a shoulder in the case of PA/ $NH_4^+$-MMTR-DI nanocomposite. This suggests a disorder in the stacking of the organosilicate layers [12], probably because of the interaction between epoxy groups and amide end groups of PA. The intercalation of PA between the organosilicate layers and the interaction with the silicate layers is also reflected in the modification of the PA crystalline structure [13]. Compared to PA (fig. 1b), characterized by a broadened diffraction maximum at 2θ = 20.12°, corresponding to δ phase (amorphous) and a diffraction maximum at 2θ =

23.6°, corresponding to α phase (crystalline) characterized by a more ordered monoclinic lattice, the nanocomposites (fig. 1) present a disorder in structure revealed by the decrease of the α form crystalline PA content and the appearance, at $2\theta = 21.5°$ of the metastable γ crystalline form (more apparently for PA/ H+-MMTR-DI nanocomposite).

The X-ray diffraction patterns for nanocomposites, obtained with the layered silicate organophilized and modified with epoxy resin, are presented in figures 1b and 1c.

The DI method leads to intercalated/partial exfoliated nanocomposites. In the nanocomposite with Cl 30 BR the basal spacing, $d_{001}$, remains unmodified as compared to Cloisite 30 B, but the diffraction peak at $2\theta = 4.8°$ decreases in intensity. This suggests a disorder in the organosilicate structure. In the nanocomposite with Cl 93 AR, the basal spacing, $d_{001}$, is 38.7Å as compared to 25.7 Å for Cloisite 93 A. Therewith, the diffraction peaks have a narrow shape and greater intensities as compared to Cloisite 93 A. These suggest that the nanocomposite obtained with Cloisite 93 AR has a more ordered structure than one obtained with Cloisite 30 BR. The MB method leads to exfoliated nanocomposites. In all the cases we observe modifications in the crystalline structure of PA even an enrichment in γ crystalline form ($2\theta = 21.38° \div 21.44°$), demonstrating the PA interactions with the silicate.

The results obtained by TGA (table 2) reveal that the nanocomposites present a much enhanced thermal stability as compared to PA. The nanocomposites decompose with maximum rate at temperatures with about 50°C higher than PA. The TGA results confirm that the masterbatch process favors the uniform dispersion of the silicate and provides higher thermal stability of the nanocomposite as a result of stronger polymer-silicate interactions.

The inorganic residue determined at 700°C provides a measure of the intercalation and/or interaction degree of PA with the silicate surface. The stronger the polymer matrix-modified-organosilicate interaction, the greater the inorganic residue value is [14].

The nanocomposites properties (table 2) are in full agreement with the TGA and X-ray diffraction results. For the nanocomposites with H+ and NH4+ montmorillonite modified with epoxy resin the decrease of the α form crystalline PA content is reflected in the lower modulus of elasticity (with 20 - 30%) and hardness (with 4 - 7%).

The strong adhesion between the polymer and silicate with uniform dispersion of the organosilicate in the polymer matrix is reflected in the increase of the modulus of elasticity. In all the nanocomposites, both the Izod Impact Strength ($A_k$) and the Flexure Strength ($\sigma_i$) decrease. The least decrease (42% - 46%) was observed in the case of PA/ Cl 93 AR nanocomposites.

The HRTEM micrographs of the selected samples confirm the morphology. With Cloisite 93 AR (fig. 2), nanocomposites with intercalated lamellar structure and intercalated/ partially exfoliated lamellar structure were obtained, respectively.

*PA/carbon nanopowder nanocomposites*

The X-ray diffraction patterns for PA/carbon nanopowder composites are presented in figure 3. In nanocomposites, in the presence of carbon nanopowder, the PA matrix suffers modification both in amorphous and crystalline structure. These results suggest the interaction between PA and carbon nanopowder (probably through the existent dangling bonds from the border of graphene layers or functional chemical groups formed during synthesis process or storage period of the carbon nanoparticles [9]).
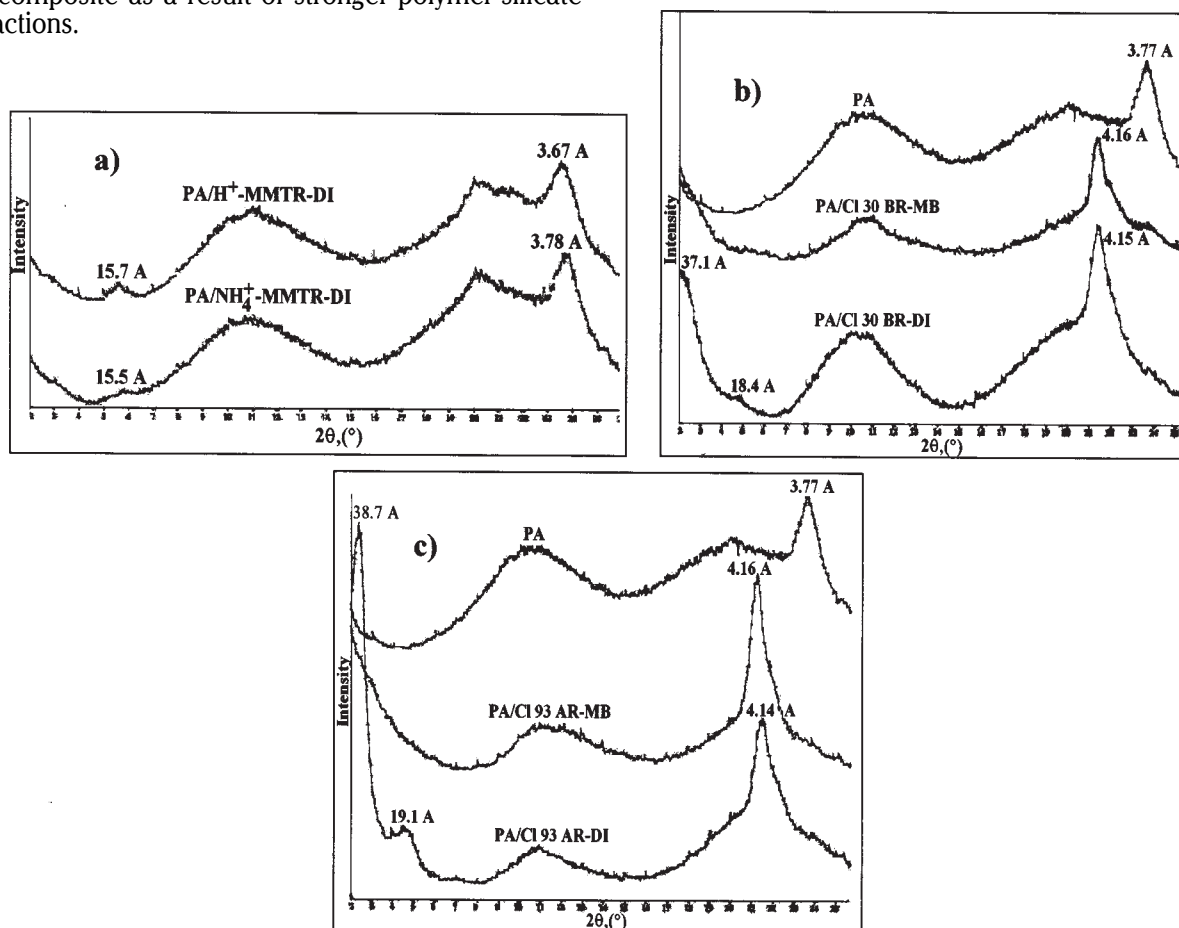


Fig. 1 X-ray diffraction patterns for: a) PA/ H+-MMTR-DI and PA/ NH4+-MMTR-DI nanocomposites; b) PA/ Cl 30 BR-DI and PA/ Cl 30 BR-MB nanocomposites and c) PA/ Cl 93 AR-DI and PA/ Cl 93 AR-MB nanocomposites

**Table 2**

THE PROPERTIES FOR THE PA/ ORGANICALLY MODIFIED LAYERED SILICATE NANOCOMPOSITES

| Crt. No. | Sample | $T_{id}$ (°C) / % loss | $T_{vd}$ (°C) | $R_{700}$ % | $E_L$ (MPa) | $D_{ShD}$ (°Sh D) | $A_k$ kJ/m$^2$ | $\sigma_i$ (MPa) |
|---|---|---|---|---|---|---|---|---|
| 1 | PA | 317/3.1 | 420 | 1.3 | 7384 | 75 | 15.2 | 98.5 |
| 2 | PA/ H$^+$-MMTR-DI | 354/2.2 | 473 | 4.4 | 7256 | 72 | 6.5 | 122.6 |
| 3 | PA/ NH$_4^+$-MMTR-DI | 343/0.02 | 466 | 6.5 | 7183 | 70 | 3.4 | 72.3 |
| 4 | PA/ Cl 30 BR-DI | 307/1.76 | 469 | 4.0 | 8513 | 75 | 4.4 | 44.1 |
| 5 | PA/ Cl 30 BR-MB | 344/2.3 | 474 | 6.7 | 8549 | 76 | 5.5 | 66 |
| 6 | PA/ Cl 93 AR-DI | 348/2.7 | 471 | 4.3 | 7759 | 74 | 8.2 | 102 |
| 7 | PA/ Cl 93 AR-MB | 352/2.2 | 479 | 7.1 | 8592 | 77 | 8.8 | 85.5 |

Note: $T_{id}$: The initial temperature of decomposition; $T_{vd}$: The temperature at the maximum rate of decomposition;

$R_{700}$: The inorganic residue at 700 °C; $E_L$: Apparent dynamic modulus of elasticity; $D_{ShD}$: Shore D hardness;

$A_k$: Unnotched Izod Impact Strength at 23°C; $\sigma_i$: Flexure Strength.
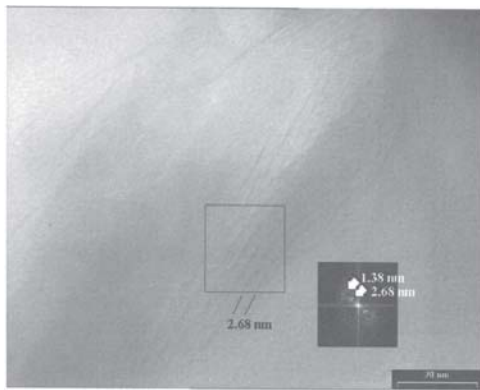


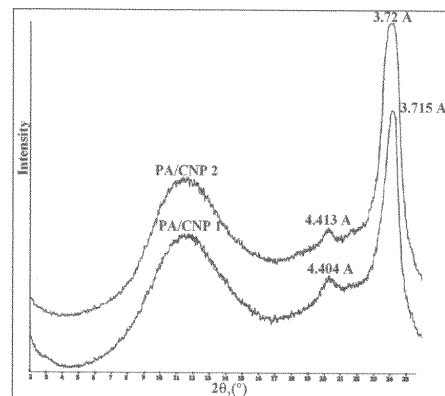Fig. 2 HRTEM image of PA/ Cl 93 AR-DI nanocomposites



Fig. 3. X-ray diffraction patterns for PA/ CNP 1 and PA/ CNP 2 nanocomposites
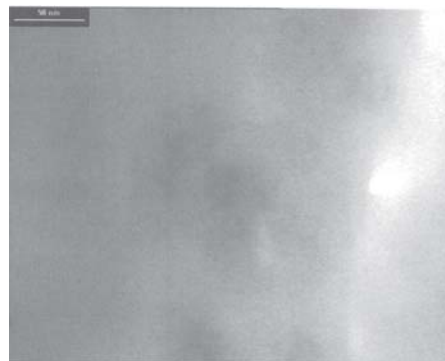


Fig. 4 HRTEM image of PA/ CNP 1nanocomposites

**Table 3**

THE PROPERTIES FOR THE PA/ CARBON NANOPOWDER NANOCOMPOSITES

| Crt. No. | Sample | $T_{id}$ (°C) / % loss | $T_{vd}$ (°C) | $R_{700}$ % | $E_L$ (MPa) | $D_{ShD}$ (°Sh D) | $\sigma_i$ (MPa) |
|---|---|---|---|---|---|---|---|
| 1 | PA/ CNP 1 | 375/2.4 | 478 | 9.7 | 8342 | 77 | 132.2 |
| 2 | PA/ CNP 2 | 385/3.5 | 476 | 5.9 | 7912 | 75 | 122.6 |

In the PA/ CNP 2 nanocomposite the PA is well crystallized and highly oriented (the diffraction peak at 2θ = 23.92° is well shaped and with very high intensity). Well crystallized but partially oriented is also the PA/ CNP 1 nanocomposite.

Carbon nanopowders enhance the thermal stability and the mechanical properties of the PA (table 3).

Higher values are obtained for the PA/ CNP 1 nanocomposite, proving a high degree of dispersion of the nanopowder in the PA matrix. In comparison with PA, the nanocomposites exhibit enhanced properties.

HRTEM micrographs on the PA/ CNP 1 confirm the uniform dispersion of the carbon nanoparticles (fig. 4).

## Conclusions

Nanocomposites based on PA and different nanofillers like onium ion, $H^+$ and $NH_4^+$ montmorillonite modified with epoxy resin and carbon nanopowder were obtained.

Nanocomposites with organically modified layered silicate having intercalated/ partially exfoliated lamellar structure were obtained by direct melt intercalation.

The direct mixing of modified layered silicate with PA results in an intercalated/partial exfoliated nanocomposite.

Masterbatch process favors the uniform dispersion of the silicate and provides higher performances of the nanocomposite as a result of stronger polymer-silicate interactions.

In the presence of the nanofiller the PA suffers modification in both amorphous and crystalline structure. These results proved the interaction between the PA and the nanofiller. In nanocomposites with carbon nanopowder the PA is well crystallized and highly oriented.

The nanocomposites exhibit heat stability and improved properties as compared to the starting material.

## References

1. HUSSAIN, F., HOJJATI, M., OKAMOTO, M., GORGA, R.E., Review article: Polymer-matrix Nanocomposites, Processing, Manufacturing, and Application: An Overview, Journal of Composite Materials, **40**, 2006, p.1511

2. VULUGA, Z., PAVEN, H., DONESCU, D., Mat.Plast., **39**, no. 1, 2002, p.19

3. MANIAS, E., TOUNY, A., WU, L., STRAWHECKER, K., LU, B., CHUNG, T.C., Chem. Mater., **13**, 2001, p.3516

4. REICHERT, P., NITZ, H., KLINKE, S., BRANDSCH, R., THOMANN, R., MULHAUPT, R., Macromol. Mater. Eng., **275**, 2000, p. 8

5. UTRACKI, L.A., KAMALL, M.R., The Arabian Journal for Science and Engineering, **27**, 2002, p.43

6. DONESCU, D., VULUGA, Z., RADOVICI, C., ŞERBAN, S., Mat. Plast., **45**, no.4, 2008, p.305

7. WANG, M.S., PINNAVAIA, T.J., Chem. Mater., **6**, 1994, p.468

8. LIU, X., WU, Q., BERGLUND, L.A., LINDBERG, H., FAN, J., QI, Z., J. of Appl. Polym. Sci., **88**(4), 2003,, p.953

9. DINCĂ, I., ŞTEFAN, A., SERGHIE, C., MOGA, A., DUMITRACHE, L., VULUGA, Z., DONESCU, D., DRAGOMIRESCU, A., PRODAN, G., CIUPINA, V., GAVRILĂ-FLORESCU, L., POPOVICI, E., SANDU, I., Applied Surface Science, **254**, 2007, p.1032

10. MORJAN, I., VOICU, I., DUMITRACHE, F., SANDU, I., SOARE, I., ALEXANDRESCU, R., VASILE, E., PASUK, I.,, BRYDSON, R.M.D., DANIELS, H., RAND, B., Carbon, **41**, 2003, p.2913

11. MORJAN, I., VOICU, I., ALEXANDRESCU, R., PASUK, I., SANDU, I., DUMITRACHE, F., SOARE, I., FLEACĂ, T.C., PLOSCARU, M., CIUPINA, V., DANIELS, H., WESTWOOD, A., RAND, B., Carbon, **42**, 2004, p.1269

12. HOFFMANN, B., DIETRICH, C., THOMANN, R., FRIEDRICH, C., MULHAUPT, R., Macromol. Rapid Commun., **21**, 2000, p.57

13. GURATO, G., FICHERA, A., GRANDI, F.Z., ZANNETTI, R., CANAL, P., Makromol Chem. **175**, 1974, p. 953.

14. ALEXANDRE, M., DUBOIS, P., Mat. Sci. and Eng., **28**, 2000, p.1